Metastable Network Model of Protein Transport through Nuclear Pores

T. Kustanovich* and Y. Rabin*†
*Department of Physics, Bar Ilan University, Ramat-Gan 52900, Israel; and †The Rowland Institute at Harvard, Harvard University, Cambridge, Massachusetts 02142 USA

ABSTRACT To reconcile the observed selectivity and the high rate of translocation of cargo-importin complexes through nuclear pores, we propose that the core of the nuclear pore complex is blocked by a metastable network of phenylalanine and glycine nucleoporins. Although the network arrests the unfacilitated passage of objects larger than its mesh size, cargo-importin complexes act as catalysts that reduce the free energy barrier between the cross-linked and the dissociated states of the Nups, and open the network. Using Brownian dynamics simulations we calculate the distribution of passage times through the network for inert particles and cargo-importin complexes of different sizes and discuss the implications of our results for experiments on translocation of proteins through the nuclear pore complex.

INTRODUCTION

The exchange of small molecules and macromolecules (proteins and ms-RNA) between the cytoplasm and the nucleus of eukaryotic cells takes place through the nuclear pore complex (NPC) by essentially two modes: whereas small molecules of <20–40 kD traverse the NPC by passive diffusion, the nuclear import of larger cargo molecules requires the formation of cargo-importin complex (CIC), which normally consists of cargo-nuclear localization signal (NLS)-importin α-importin β (for reviews see Chook and Blobel, 2001, Macara, 2001, Rout and Aitchison, 2001, Vasu and Forbes, 2001, and Suntharalingam and Wente, 2003). Upon its formation in the cytoplasm, the CIC translocates through the NPC and dissociates in the nucleus (translocation of large cargo in the reverse direction requires exportins and nuclear export signals). This process is both highly selective and efficient; it can accommodate transport of up to 1000 cargoes per NPC per second (Ribbeck and Görlich, 2001). Experiments suggest that the central core of NPC has a compact organization, in which nucleoporin proteins, or Nups, make contacts with each other, creating a barrier that restricts the passive diffusion of gold particles with diameters exceeding 8 nm. The passage of CIC through the NPC is believed to occur by facilitated diffusion involving the repeated binding and dissociation of CIC from nucleoporins that form the NPC (there are ~30 different types of Nups, with average 100 kD mol wt per Nup).

Most models for translocation of cargo-importin complexes through the NPC assume that it involves binding (possibly due to hydrophobic interactions) between importin-β and FG (Phe-Gly) repeats that are present in nearly half of the nucleoporins that form the core of the NPC. Early models of translocation assumed opening and closing of the central channel of the NPC by ATP-driven mechanochemical means in response to signal sequences (see review by Chook and Blobel, 2001). However, these models were later abandoned due to emerging evidence that the translocation process itself does not require energy (Schwoebel et al., 1998; Englmeier et al., 1999) and that hydrolysis of GTP in the cytoplasm and exchange of RanGDP by RanGTP in the nucleus, is required only to regulate the formation and the dissociation of the cargo-importin complex and ensure the directionality of the process (it has been suggested that the directionality can be changed by reversing the RanGTP gradient; see Nachury and Weis, 1999).

Present day models fall broadly in one of two classes, i.e., those that focus attention on the process of entry into the NPC and those that consider the motion of cargo through the central core of the NPC. Thus, in the affinity gating scenario (Rout et al., 2000), the entry of large inert cargoes into the cytoplasmic end of the NPC is blocked by filamentous FG Nups. Once the CIC is formed, the binding of importin-β to these Nups increases the probability of entry into the central core of the NPC and, from that point on translocation proceeds by simple Brownian diffusion. Although such a mechanism is likely to promote selective translocation, it has been argued that initial NPC entry alone is not sufficient for the translocation of large cargoes and that the major barrier to diffusion lies within the central region of the NPC (Lyman et al., 2002).

According to the selective phase model (Ribbeck and Görlich, 2001), FG-rich Nups associate to form a barrier meshwork (a sieve-like structure) within the core of the NPC, possibly through hydrophobic interactions between FG repeats. Passage of objects larger than the mesh size requires local ''breaking'' of the network by its attachment to FG binding sites on importin-β that compete with the binding between Nups. Such a mechanism allows the CIC to ''dissolve'' into the sieve. The model assumes low affinity Nup-Nup and Nup-CIC interactions, consistent with the observation that high-affinity interactions usually imply small dissociation rates that are incompatible with the observed fast translocation rates. Notice, however, that the naive interpretation of the above model in terms of a network of

Submitted September 9, 2003, and accepted for publication November 5, 2003.

Address reprint requests to Professor Yitzhak Rabin, E-mail: rabin@mail.biu.ac.il.

0006-3495/04/04/2008/09 $2.00

weakly bound hydrophobic repeats is inconsistent with the observed selectivity, because such a transient network would open and close due to thermal fluctuations, and therefore will allow translocation of cargo even in the absence of importins. Also, it has been argued that a macromolecule that can attach to the network will have a lower, not higher mobility than an inert one that does not form such attachments (Bickel and Bruinsma, 2002). Interestingly, our preliminary results obtained after this paper was submitted for publication show that if only chain-CIC but not chain-chain attractive interactions are allowed (i.e., the network is completely dissociated but chains can have short-lived bonds with the CIC), varying the number of binding sites per chain from zero to four does not affect the distribution of translocation times.

In this work we attempt to resolve an apparent paradox that confronts network models of translocation through the NPC: how could it be possible that a protein that is too big to pass through the network by simple diffusion, puts on a coat of NLS+importin-α+importin-β the thickness of which can far exceed its original dimensions and then, without any expenditure of energy, traverses the meshwork at a rate with which it would diffuse in an unrestricted liquid medium with the viscosity of the cytoplasm (Ribbeck and Görlich, 2001)?! The mystery disappears if one assumes that the importin complex acts as a catalyst that lowers the free energy barrier between open and closed states of the network (Stryer, 1995) and allows any object with dimensions smaller than the diameter of the central transporter region of the NPC to pass through. The fact that the network is impermeable to inert objects with dimensions larger than the mesh size means that the free energy barrier between end-linked and dissociated states is much larger than k_BT (k_B is the Boltzmann constant and T the temperature). Furthermore, the observation that GTP hydrolysis is not required for a single pass through the NPC, implies that these bound and open states of the network have nearly the same free energy, i.e., that the binding energy between FG Nups is compensated by entropy losses (a simple model based on the balance of attraction and tension is presented below; see also Bickel and Bruinsma, 2002). Notice that if the above suggestion of small free energy difference between the bound and the free states of two FG Nups is correct, the corresponding nucleoporins will exhibit low equilibrium affinity for each other. This statement appears to be consistent with nucleoporin affinity capture experiments in which no mobile FG Nups were observed to be captured by immobilized FG Nups, possibly because the affinities were too low to be detected by this method (Allen et al., 2001).

THE METASTABLE NETWORK MODEL

A measurable characteristic of the translocation process is the average rate of passage through the NPC (Peters et al., 2003). Its inverse, the mean passage time, is the sum of time it takes the translocating object to enter and exit the pore and the passage time through the hypothetical Nup network that blocks the free diffusion of large objects through the central core region of the NPC. Because, for objects with size comparable to or larger than the average mesh size, one expects that the rate-limiting process is the passage through the network, in the following we focus on this part of the translocation process and disregard issues concerning the cytoplasmic entry into and the nucleoplasmic exit from the NPC. In lieu of direct experimental information about the structure of this network, our model assumptions are dictated mainly by considerations of simplicity and computational feasibility. Thus, instead of considering a thick layer of FG Nups attached to the walls of the NPC core, we model the NPC as a long pore whose center is blocked by single layer that contains 16 polymers (this choice is consistent with the eightfold symmetry of the NPC). Every polymer is grafted by one end to the wall of the pore and its other end can be either attached to that of another polymer (end-linked) or free (dissociated). For simplicity, we assume that each chain has a single attachment (binding) site located at its free end, and that only pairwise associations between chains that are grafted to the wall diametrically opposite to each other are allowed. Typical configurations of the fully cross-linked and the fully dissociated network are shown in Fig. 1, *a* and *b*, respectively. Notice that even though the average mesh size is completely determined by geometry, the instantaneous mesh size at each position in the network fluctuates in time because the chains are end-linked and there are no real cross-links at the intersections of the lines in Fig. 1 *a* (which, in fact, are not true intersections but only projections of three-dimensional configurations of the chains on the plane of the cross section).

We assume that the end-linked and the free states of a chain are separated by a large free energy barrier ($\gtrsim$10 k_BT per polymer, a value intermediate between thermal energy and the energy of a covalent bond) that guarantees that spontaneous dissociation of end-links does not take place on timescales relevant to the translocation process, thus ensuring that inert cargoes with dimensions larger than the mesh size do not pass through the network. As

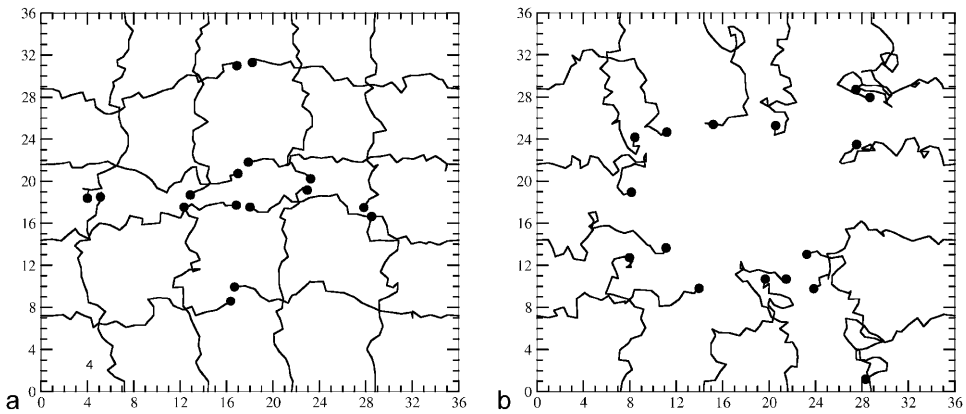

FIGURE 1 A snapshot of network fluctuations (*a*) and of the grafted chains (*b*) at $T = 0.3$. The beads shown are those with *c*-*c* (chain-chain) interaction.

proposed by Bickel and Bruinsma (2002), such a metastable free energy landscape may arise as the result of balancing the large but localized binding energy between two FG Nups, against the loss of elastic entropy associated with the stretching of the chains compared to their equilibrium dimensions (compare Fig. 1, *a* and *b*). A schematic example is shown in Fig. 2 where we plot the free energy of a chain as a function of the distance r of its free end from the wall: the binding contribution is represented by a narrow and deep square well potential centered about the middle of the channel, and the elastic entropy contribution due to stretching is given by the parabolic curve (de Gennes, 1979).

The presence of the energy barrier does not affect the equilibrium ratio of end-linked to dissociated polymers, which is determined only by the small free energy difference between the two equilibrium states and, in general, we would expect a significant fraction of end-links to be dissociated at any particular moment. Therefore, to simulate the above network, one should allow the polymers to reach equilibrium in which they slowly fluctuate between their free and bound states. Because in this simulation we considered a single-layered network consisting of only 16 polymers, such a procedure would lead to large fluctuations of the instantaneous fraction of bound chains and thus of the effective mesh size. Although larger equilibrium systems will be studied in the future, in this work we circumvent the small system limitations by disregarding the equilibrium fraction of free chains and begin each simulation cycle with a fully connected network (see Fig. 1 *a*). As already mentioned, the height of the free energy barrier that separates the end-linked and the dissociated states is sufficiently high so that spontaneous dissociation does not take place on timescales relevant to translocation through the layer. Thus, the only objects larger than the average mesh size that can pass through the layer are those that can catalyze the dissociation of Nup-Nup bonds by binding to FG repeats and locally disrupt the Nup network, detach from it, and diffuse away.

The above assumptions define the metastable network model used to simulate the passage of a tracer particle that represents an inert cargo or a CIC through the NPC. The tracer is taken to be a spherical particle of effective radius R_t and, in the case of a CIC, it has N_t ''binding'' sites each of which represents a Nup binding site of importin-β. To save computational time and to introduce the vectorial character of translocation into the model, the tracer is subjected to a weak force (F^z_{tracer}) directed along the channel that gives it a nonvanishing longitudinal velocity (in the absence of a network). We would like to stress that the above force is introduced solely to speed up the calculation and does not represent a physical force acting on the translocating object. However, thermodynamic driving forces may indeed arise in experiments, as the result of chemical potential and/or concentration gradients between the cytoplasm and the nucleoplasm (Ribbeck and Görlich, 2001).

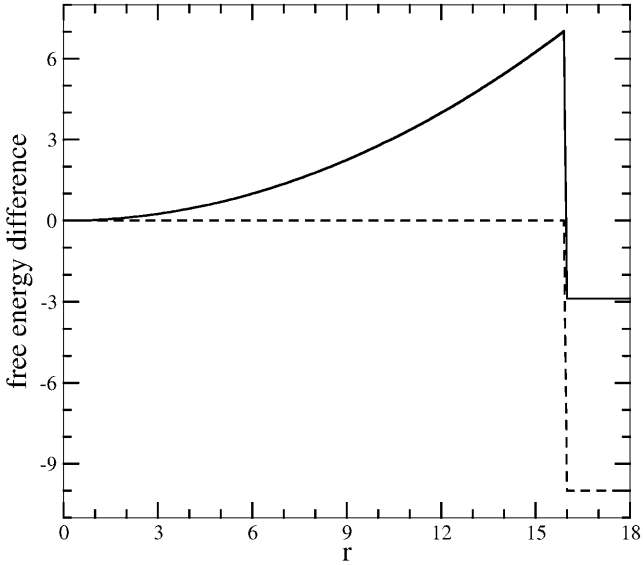

FIGURE 2 The free energy of a chain versus the distance r of its free end from the wall. The combined contribution from the binding energy due to *c-c* interactions (*dashed line*) and from the elastic entropy (a parabolic *curve*) is given by solid line. Notice that the barrier height is much higher than the equilibrium binding free energy.

The modeling of Nups is based on the observation that they possess high flexibility and low compactness (Denning et al., 2003), and therefore can be described by the standard model of polymers as linear chains of beads connected by elastic springs. Such chains are often simulated by finitely extensible nonlinear elastic (FENE) potential (see e.g., Grest and Kremer, 1986 and Kremer and Grest, 1990)

$$U_{\text{FENE}}(r) = -\frac{1}{2}k_0 r_0^2 \ln(1 - r^2/r_0^2). \tag{1}$$

In the simulations we used the values $k_0 = 60$, and $r_0 = 1.8$ (the motivation for this particular choice of parameter values is discussed in the following). To balance this attraction and to take into account the excluded volume repulsion between beads belonging either to the same or to different chains, a short-range Lennard-Jones (LJ) potential

$$U(r) = 4\varepsilon\left[\left(\frac{\sigma}{r}\right)^{12} - \left(\frac{\sigma}{r}\right)^{6} + \frac{1}{4}\right], \tag{2}$$

with $r < 2^{1/6}\sigma$ is used (note that because the minimum of the above potential is at $r = 2^{1/6}\sigma$, the potential is purely repulsive in this range). Taking the effective bead radius to be 1/2 (all lengths and temperature are in reduced LJ units, with Boltzmann constant $k_B = 1$), $\sigma^{bb} = 1$ describes the characteristic distance of bead-bead repulsion, denoted U^{bb}.

Consistent with the metastable network model, the *c-c* (chain-chain) attraction between binding sites belonging to different chains is chosen to be stronger than the Brownian force due to thermal fluctuations. At small distances this attraction is balanced by short-range repulsion, so that two binding sites would not come too close together and cause breakage of intrachain (FENE) bonds. To simulate the interaction between FG-rich regions on different Nups, we used the LJ potential U^{cc}, Eq. 2, with parameters: $\varepsilon^{cc} = 6$, $\sigma^{cc} = 1.2$, and interaction range $r^{cc} \le 3\sigma^{cc}$ (this potential is attractive in the range $2^{1/6}\sigma^{cc} < r^{cc} \le 3\sigma^{cc}$). This choice guarantees that the network remains stable under thermal fluctuations at the temperature $T = 0.3$ used in the simulation (with this choice of temperature $\varepsilon^{cc} = 20\,k_BT$). Notice that although there is a jump of the potential at the cutoff, its magnitude is an order of magnitude smaller than k_BT and therefore it does not affect our simulation results (a similar comment applies to tracer-chain interactions introduced below). Thus, for bead i participating in the *c-c* interaction, the interaction potential U_i is

$$U_i = \sum_l U_{\text{FENE}} + \sum_j U^{bb} + \sum_k U^{cc}, \tag{3}$$

where l denotes the neighboring beads along the chain contour that are connected to bead i. The index j goes over all beads (of the same or different chains) that are close to bead i, and k denotes beads on other chains that have an attractive interaction with bead i. All the sums are taken over pairs only and no interactions are double counted. The binding site of each chain (the bead located at its end) can form a *c-c* bond with another chain or form a *c-t* (chain-tracer) bond with one of the N_t binding sites on the tracer. The diameter of the channel (the characteristic dimension of the cross section in the *X-Y* plane) and the mesh size of the network determine the size of inert and interacting tracers that could pass through. Assuming a square cross section of size L, the average mesh size is $\xi = L/(N_c/4 + 1)$, where N_c is the number of chains in the meshwork ($N_c/4$ is the number of chains grafted to each of the sides of the cross section). Another relevant parameter is the number of beads in a chain N_b, which determines the root mean square end-to-end distance of a chain R_c (de Gennes, 1979):

$$R_c \approx \sigma^{bb} N_b^{0.6}. \tag{4}$$

For $L \gg R_c$ the network consists of strongly stretched chains. This guarantees that once the attachment between the chains is broken by the tracer, they recoil and do not recombine on the timescale of its passage through the network (an instantaneous realization of a fully dissociated network is shown in Fig. 1 *b*). We used the values $L = 36$, $N_b = 30$, and $N_c = 16$. The top of the channel is located at $Z = 50$, its bottom at $Z = 0$, and the chains are permanently attached to the wall at the plane $Z = 18$.

In our simulations the tracer is introduced at the top of the channel and its center of mass undergoes Brownian motion in the presence of a weak downward force (F^z_{tracer}) until it reaches the bottom of the channel. We assume that only the center of mass of the tracer is moving (for simplicity, rotation is not taken into account). The excluded volume between its center of mass and any nearby bead on a chain, U^{tc}_{ev}, is modeled by repulsive LJ interaction, Eq. 2, with $\varepsilon^{tc}_{ev} = 1$ and $\sigma^{tc}_{ev} = R_t + 0.5$. For spherical tracers of radius R_t that represent the CIC, N_t equally spaced binding sites are located on a circle drawn on the surface of the sphere. The plane of the circle is parallel to the *X-Y* plane (because the sphere is not allowed to rotate, this plane is fixed during the translocation process), and is at a distance 2 from the bottom of the sphere. We used $N_t = 6$ and $R_t = 4, 8$ for CIC tracers, and $N_t = 0$ and $R_t = 3, 3.5, 4$ for inert ones. In the beginning of each simulation cycle (see details in Appendix A), the coordinates X_t and Y_t of a tracer are randomly chosen from the interval $[1 + R_t, L - 1 - R_t]$ while $Z_t = 48 - R_t$. The tracer is free to diffuse in the *X-Y* plane (it bounces from the walls), but is subject to constant force acting on its center of mass, which pushes it downward in the *Z* direction. Using $F^z_{tracer} = 0.5$ ensures that the force is small enough so that an inert tracer cannot break the network. Each cycle ends at $Z_t = R_t$.

The assumption that the CIC can catalyze the breaking of a *c-c* bond by first replacing it with a *c-t* bond and then dissociating from the chain, suggests that the strength of chain-tracer interaction can be modeled by $D\varepsilon^{cc}$, where D is random function of time. The lower and the upper bounds on D are set by observing that for competing with *c-c* interaction it is enough to have $D \approx 1$, whereas for efficient dissociation one must have $D \leq k_BT/\varepsilon^{cc} \ll 1$. This guarantees that *c-t* bonds have a finite lifetime and therefore, that the CIC acts as a catalyst that returns to its original state after the dissociation reaction is completed. Consistent with the above, in the simulation we randomly choose D_i for each binding site i on the tracer, from a uniform distribution in the interval [0, 1]. Another important factor is the rate at which D_i is chosen. We found that making an independent choice of D_i every 10 time steps, guarantees that the *c-t* bond persists for a sufficiently long time. This allows the other chain end to move away and prevents recombination of *c-c* bonds that remain open long enough for a tracer to move through the network.

To model the competition between chain-chain and tracer-chain attractions, we used the following simplified scenario. When a binding site k on a tracer approaches an existing c_i-c_j bond, there is a competition between the three binary interactions, c_i-c_j, c_i-t_k, and c_j-t_k, with the ''winner'' defining the new bond. The estimation of the effective *c-c* and *c-t* interactions is performed in two steps: First, the strength of the three bonds is calculated

$$F^0_{mn} = -AU'(r_{mn}), \tag{5}$$

where m, n represent *c-c* and *c-t* bonds, $A = 1$ for chain-chain interaction, and $A = D$ for chain-tracer interaction. If one (or more) of $F^0_{mn} > 0$, the interaction is repulsive and in this case the strength of the interaction is not modified in the next step, i.e., $F^1 = F^0$. Most of the time, however, all interactions are attractive. Assuming that the strongest attraction between c_i-c_j, c_i-t_k, and c_j-t_k defines the ''winning bond'', we rescale the interactions according to

$$F^1_{mn} = \alpha F^0_{mn}, \tag{6}$$

where $\alpha = 1$ for $F^0_{mn} = \max(|F^0_{ij}|, |F^0_{ik}|, |F^0_{jk}|)$ and $\alpha = 0.5$ in the other cases. The force acting on site m is thus given by

$$\vec{F}_m = \sum_n \vec{F}^1_{mn}. \tag{7}$$

RESULTS

Typical instantaneous configurations of inert tracers (IT) and of cargo-importin complexes (CIC) of different sizes as they pass through the network are shown in Figs. 3 and 4. In Fig. 5 we plot the distribution of rates of passage of IT with diameters close to the average mesh size $\xi = 7.2$. As expected, the rate decreases steeply as the dimensions of the tracer approach the mesh size and whereas IT with $R_{IT} = 4$ can still get through due to fluctuations of the instantaneous mesh size, the translocation of larger IT is practically arrested (for $R_{IT} \geq 5$ no passage events were observed during time $t = 5000$). These results are consistent with the observation of Ribbeck and Görlich (2001), that whereas unfacilitated diffusion through the NPC of a GFP protein with radius 2.36 nm is slowed down by a factor of 100 compared to its diffusion through the cytoplasm, the diffusion of larger BSA proteins with radius 3.55 nm is slowed down by a factor of 1000. The shapes of the distributions resemble those reported for the passage of small dextran molecules (4, 10, and 20 mol wt) through microarrays of small nuclear envelope patches (Keminer and Peters, 1999), even though direct comparison of our simulation of rigid tracers with experiments on flexible polymers cannot be done (the kinetics and the mechanism of translocation of the latter is quite different; see Salman et al., 2002). Typical configurations of CIC (each with six interacting sites) during various stages of opening and passage through the network, with $R_{CIC} = 4$ and $R_{CIC} = 8$, are shown in Figs. 3 *b* and 4, respectively. The statistics of passage times in the various cases is summarized in Table 1.

Inspection of Table 1 and of the histogram in Fig. 6 shows that the catalytic effect of interacting sites has a dramatic effect on the distribution of passage times, even for tracers (e.g., with $R_t = 4$) that are small enough for unfacilitated passage through the network. For such tracers, the most probable passage time is nearly the same for IT and for CIC; however, in the former case the distribution is extremely broad and the mean passage time is more than three times larger than that of the corresponding CIC. The latter observation agrees with experiments that report that even though GFP (a small protein with 28 kD mol wt) can pass unaided through the NPC, it translocates much slower on the average than NTF2 which is an importin-type protein of comparable size (Ribbeck and Görlich, 2001; Siebrasse and Peters, 2002).

Fig. 7 reveals another interesting aspect of facilitated translocation of CIC predicted by our simulation. Unlike the very broad distribution of passage times observed for IT with $R_t = 4$, the corresponding distributions for CIC with radii 4 and 8 are quite narrow, and although the peak of the distribution moves toward higher passage times approximately linearly with size, the shapes of the two distributions are quite similar.

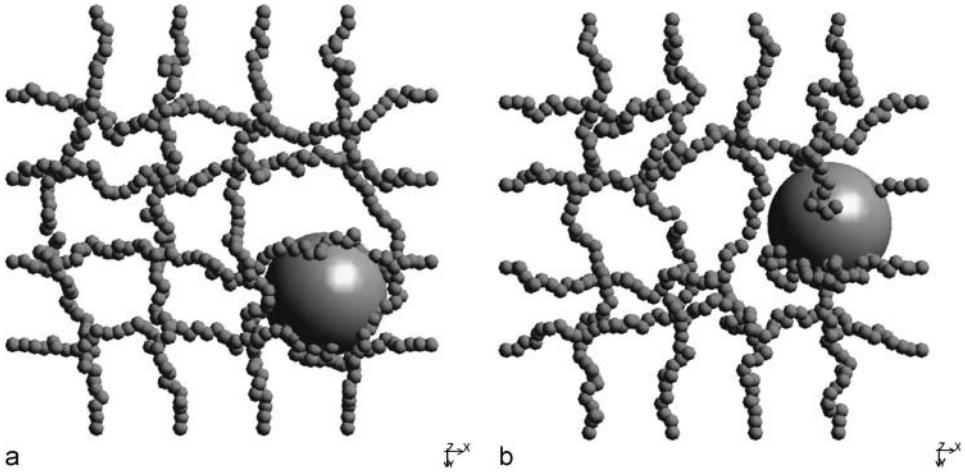

FIGURE 3 An IT (*a*) and CIC (*b*) with $R_t = 4$ can pass through the network, the former due to thermal fluctuations (in a fully connected network $\xi = 7.2$) and the latter by also locally breaking the mesh.

Finally, we examine the size limit on translocation of inert tracers imposed by the diameter of the channel and the equilibrium dimensions of the grafted chains (FG Nups). In Table 2 and Fig. 8 we present the statistical properties and the histograms of passage times of IT that move through a fully dissociated network shown in Fig. 1 *b*. Inert tracers with $R_t = 4$ and 8 can easily pass through the open channel, resulting in narrow distributions of passage times (Fig. 8 *a*). The very broad distribution of passage times of an IT of $R_t = 12$ (Fig. 8 *b*) stems from the fact that for chains with equilibrium dimensions $R_c \simeq 7.7$ used in the simulation, the effective diameter of the open channel is smaller than the diameter of the tracer ($L - 2R_c < 2R_t$), which can therefore pass through the layer only due to fluctuations of the chains.

CONCLUSIONS

We have presented the results of computer simulations of the metastable network model of translocation of proteins through nuclear pores. Although several of the underlying assumptions of this model are clearly speculative, the simplicity of the model allows one to explore its consequences in detail. Let us briefly review the logical structure of the model. We begin by assuming that the central core of the NPC is blocked by a network, formed by attractive interactions between FG Nups. The mesh size of this network determines the observed upper cutoff on the size of objects (proteins, gold particles) that can pass through it by passive diffusion. For this model to work one has to assume that the network is practically irreversible under normal conditions. The next step comes from the observation that larger cargo that would not be able to translocate through the NPC, does not experience significant barriers to diffusion when bound to importins. This suggests that importins are the source of the ''magic'' that opens the network and allows the CIC to move through it. If, as appears to be the consensus in the field, the process of passage does not require hydrolysis of GTP, importins (i.e., importin-β) act as catalysts that reduce the free energy barrier between the cross-linked and the free states of the network, dissociating the bonds between the Nups that form it.

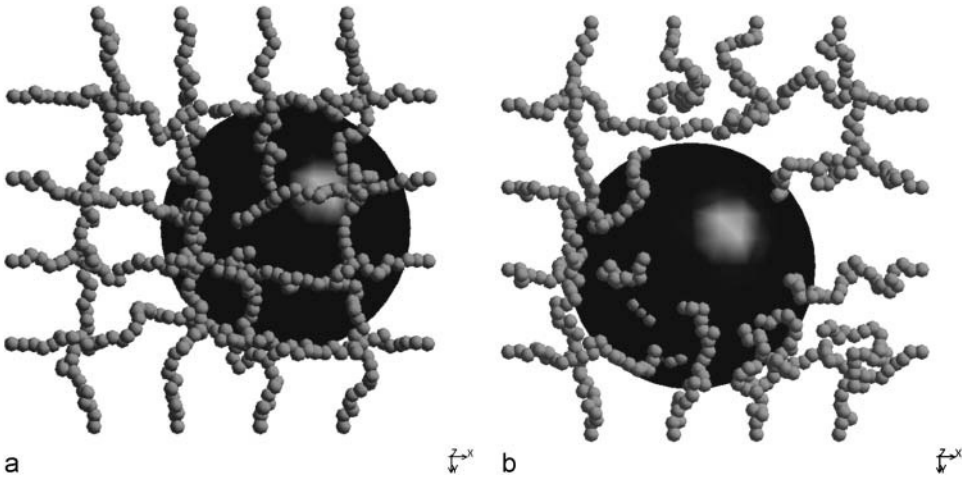

FIGURE 4 CIC with $R_t = 8$ passes through the network by breaking it.

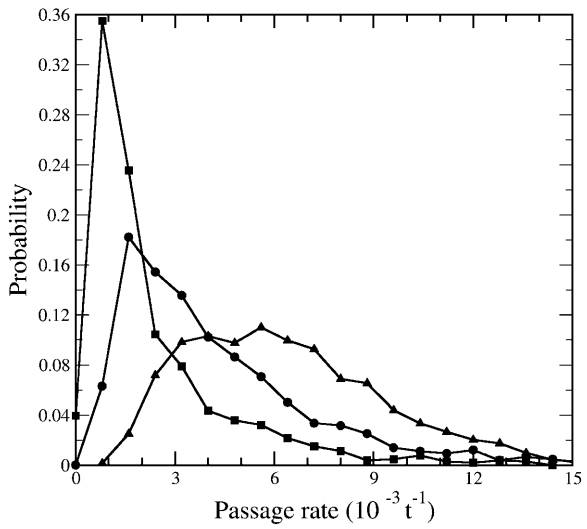

FIGURE 5 Histogram of passage rates of IT with $R_t = 3$ (▲), $R_t = 3.5$ (●), and $R_t = 4$ (■). The passage rate is given in units of $(1000 \times t)^{-1}$.

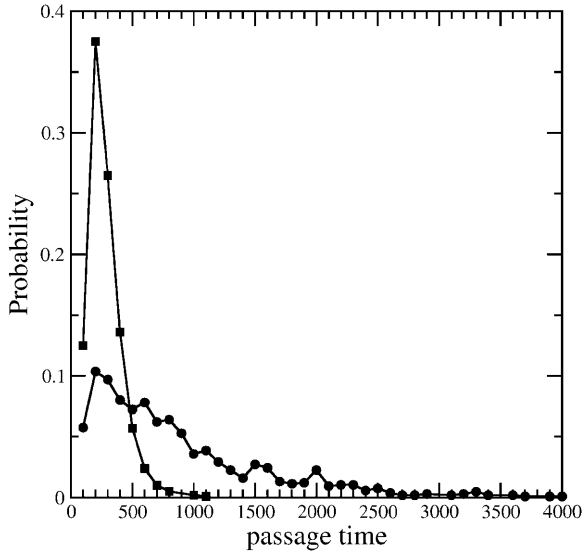

FIGURE 6 Histogram of passage times of IT (●) and CIC with $N_t = 6$ (■), both of size $R_t = 4$.

In addition to the above-discussed main assumptions of the metastable network model, other assumptions are made as well, for reasons of simplicity and concreteness. For example, we postulate that the network consists of a single layer of Nups. In reality, there may be several layers whose presence plays an important role in releasing the *c-t* bonds and allowing the CIC to propagate forward. Such a picture would be consistent with the results of Ben-Efraim and Gerace (2001), who found that there is progressively increasing affinity of importin-β for certain nucleoporins along the pathway of nuclear import. This raises the possibility that the transport of CIC between two nucleoporins (as it moves across a multilayered network) may involve at least two distinct interaction sites for the importin-β with nucleoporins: the binding of an importin-β to one nucleoporin becomes transient, as this binding site is released upon interaction of importin-β with a second nucleoporin. Moreover, additional factors, such as RanGTP could promote transfer/release reactions, possibly utilizing the allosteric character of the importin β–RanGTP complex, recently reported by Nevo et al. (2003).

Another simplification used in our simulation is that each simulation cycle begins with a tracer particle introduced above a fully cross-linked layer and ends after the particle has passed to the other side of the layer. In principle, the ''hole'' in the network catalyzed by the passage of CIC will remain open for some time after the translocation event. This suggests experiments on mixtures of CIC and inert tracers that would check whether the presence of the former facilitates the translocation of the latter.

The implementation of the catalytic activity of the CIC in our model through a step-like process that consists of replacing chain-chain bonds by chain-tracer ones and breaking the latter at random, is a major oversimplification. This is unavoidable because at present there is no microscopic understanding of the interaction between importin-β and FG Nups. The only knowledge about these interactions

TABLE 1 Statistics of passage times through the network

System	Mean time	Standard deviation	Most-probable time	# of cycles
$R_{IT} = 3$	200	120	120	1436
$R_{IT} = 3.5$	540	310	170	1076
$R_{IT} = 4$	900	800	240	1062
$R_{CIC} = 4$	280	130	210	1000
$R_{CIC} = 8$	530	160	440	1061

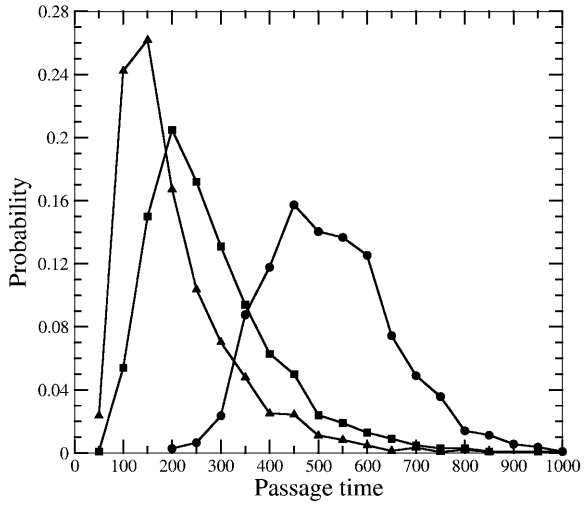

FIGURE 7 Histogram of passage times for IT with $R_t = 3$ (▲), and for CICs with, $R_t = 4$, $N_t = 6$ (■); and $R_t = 8$, $N_t = 6$ (●).

TABLE 2 Statistics of passage times through an open channel

System	Mean time	Standard deviation	Most-probable time	No. of cycles
$R_{IT} = 4$	170	90	150	1200
$R_{IT} = 8$	280	80	250	1200
$R_{IT} = 12$	2100	1400	1300	1135

comes from indirectly related observations, e.g., that the complex of some Nups with the yeast analogue of the CIC is unexpectedly short-lived (Gilchrist et al., 2002). Another, possibly relevant result was reported by Nevo et al. (2003), who showed that the Ran–importin β complex has an allosteric character. Interestingly, Ran may also play an important role in the catalysis of *c-c* bonds by CIC. It was shown (Lyman at al., 2002) that there are different requirements for the translocation of small and large CIC: whereas efficient import of three different proteins with molecular weight in the range 60–125 kD was supported by Ran and non-hydrolyzable GTP, nuclear import of two larger cargo proteins with 500 kD mol wt and 669 KD mol wt required both Ran and GTP. The authors suggested that CIC movement through the central channel of NPC can be explained by a modified facilitated diffusion model in which RanGTP plays a role that depends on both cargo size and the avidity of the CIC for FG Nups. CIC (whether large or small) with small avidity for FG Nups have a small probability of reassociating with a particular Nup after dissociating from it and therefore will be able to migrate through the NPC. In the case of CIC with large avidity for nucleoporins, such reassociation events would stall transport of larger receptor-cargo complexes (with small diffusion coefficients) that have a low probability of escaping from one nucleoporin after dissociating from it and, therefore, would tend to reassociate with the same Nup. Smaller CIC can dissociate and move away sufficiently fast, which would allow them to bind to a different nucleoporin rather than being recaptured by original binding site, and thus to transit the NPC by multiple binding/dissociation cycles. According to the above model, binding of RanGTP to importin-β plays a dual role; it promotes the dissociation of the CIC-Nup complex and prevents rapid reassociation by weakening the affinity of CIC for FG Nups (the latter was shown by Rexach and Blobel (1995)), thus allowing even larger CIC to diffuse away. Although our model has no explicit reference to Ran, its effect on the probability of reassociation of CIC and Nups can be simulated by tuning the magnitude and the statistical properties of the interaction between them.

In summary, in this work we have constructed a model of translocation of inert tracers and cargo-importin complexes through the NPC. The simplifications and approximations used are such that this model can only predict qualitative trends and cannot be used for quantitative comparison with experiment. We calculated the distribution of passage times and studied its dependence on the size of the translocating object and on the presence of catalytic (attractive) sites on its surface. We showed that there is an abrupt upper cutoff on the size of inert particles that can translocate through the network and that this cutoff is somewhat bigger than the average mesh size of the network. We found that inert tracers and CIC with identical diameters approaching this cutoff have similar most-probable times of passage through the network but that the mean time of passage of the latter is much smaller than that of the former. Although a detailed study of the dependence of the passage time on the number of sites/tracer size ratio is deferred to future work (because of the need to accumulate statistics, these simulation runs took several months on a small cluster of state-of-the-art PCs), our preliminary results comparing $N_t = 1$ with $N_t = 6$ concur with the observation that increasing the number of impor-

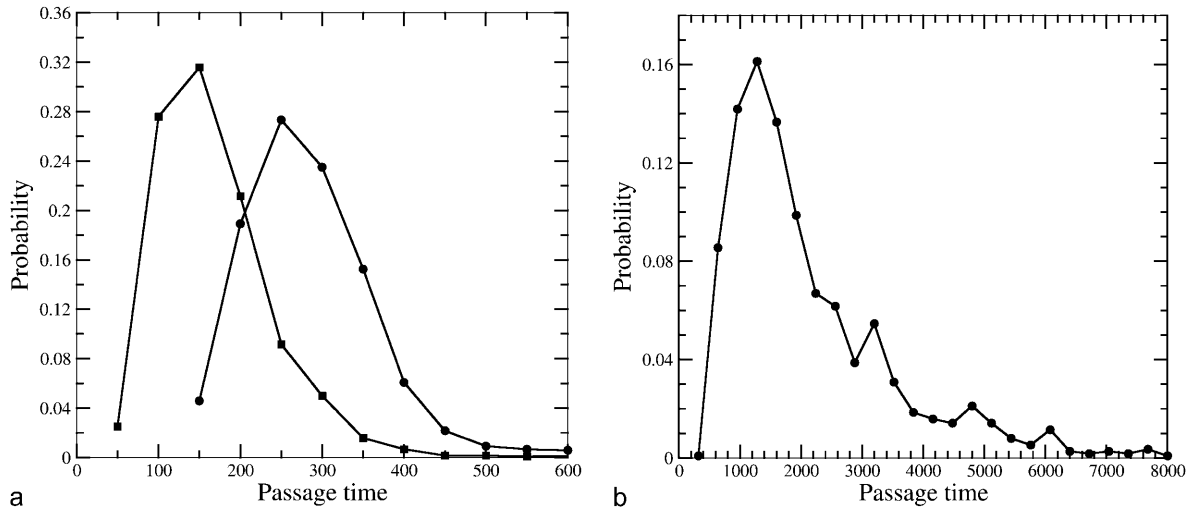

FIGURE 8 Histogram of passage times for IT with (*a*) $R_t = 4$ (■) and $R_t = 8$ (●), and (*b*) $R_t = 12$ through an open channel. Notice the difference of timescales in Fig. 8, *a* and *b*.

tins bound to a cargo increases the efficiency of transport (Ribbeck and Görlich, 2002).

APPENDIX A: SIMULATION DETAILS

The motion of the chains and of the center of mass (c.m.) of the tracer is performed using a standard Brownian dynamics algorithm (see, e.g., Allen and Tildesley, 1987). Each bead of the chains (tracer) moves according to the equation of motion (bead and tracer mass is taken as unity):

$$\ddot{\vec{r}}_i = \vec{F}_i - \Gamma\dot{\vec{r}}_i + W_i(t), \tag{A1}$$

where Γ is the bead (tracer) friction coefficient (we used $\Gamma = 0.5$) and $W_i(t)$ describes the random force of the heat bath acting on each bead (tracer):

$$\langle W_i(t) \cdot W_j(t')\rangle = \delta_{ij}\delta(t-t')6k_BT\Gamma. \tag{A2}$$

The force on bead i is given by

$$\vec{F}_i = -\nabla\left(\sum_l U_{FENE} + \sum_j U^{bb} + U^{wall}\right) + \delta_{im}\vec{F}_m, \tag{A3}$$

where U^{wall} is a repulsive LJ potential, Eq. 2, with parameters: $\varepsilon^{wall} = 1$, $\sigma^{wall} = 1.0$, and the δ-function δ_{im} ensures that $\vec{F}_m$, Eq. 7, acts only on beads participating in c-c (c-t) interaction.

The force on the c.m. of tracer is given by

$$\vec{F}_i = -\nabla\left(\sum_l U_{ev}^{tc} + U^{wall}\right) + \delta_{im}\sum_{m=1}^{N_t}\vec{F}_m + F^z_{tracer}\hat{z}, \tag{A4}$$

with $\vec{F}_m$, Eq. 7, acting on interacting sites of the tracer. As described in the text, we introduced a weak auxiliary force that acts on the tracer downward in the Z direction ($\hat{z}$ is a unit vector along the Z axis), $F^z_{tracer} = 0.5$.

The Brownian dynamics is preformed using Verlet-like algorithm (see, e.g., Chapter 9, Allen and Tildesley, 1987):

$$\begin{aligned}\vec{r}(t+\delta t) &= \vec{r}(t) + c_1\delta t\vec{v}(t) + c_2\delta t^2\vec{a}(t) + \delta\vec{r}^G\\ \vec{v}(t+\delta t) &= c_0\vec{v}(t) + (c_1 - c_2)\delta t\vec{a}(t) + c_2\delta t\vec{a}(t+\delta t) + \delta\vec{v}^G,\end{aligned} \tag{A5}$$

with

$$c_0 = e^{-\Gamma\delta t}; \quad c_1 = (1-c_0)/(\Gamma\delta t); \quad c_2 = (1-c_1)/(\Gamma\delta t).$$

In the simulation, each pair of vectorial components $\delta\vec{r}^G$ and $\delta\vec{v}^G$ is sampled from a bivariate Gaussian distribution:

$$\begin{aligned}\delta r_\mu^G &= \eta_1\sigma_r\\ \delta v_\mu^G &= (c_{rv}\eta_1 + \sqrt{1-c_{rv}^2}\eta_2)\sigma_v,\end{aligned}$$

where η_1 and η_2 are two independent normal random variables, with zero means and unit variances, and

$$\begin{aligned}\sigma_r &= \{(\delta t k_BT/\Gamma)[2 - (3 - 4e^{-\Gamma\delta t} + e^{-2\Gamma\delta t})/(\Gamma\delta t)]\}^{0.5}\\ \sigma_v &= \left[k_BT(1 - e^{-2\Gamma\delta t})\right]^{0.5}\\ c_{rv} &= k_BT(1 - e^{-\Gamma\delta t})^2/(\Gamma\sigma_r\sigma_v).\end{aligned}$$

We used $\delta t = 0.01$ to prepare independent samples of the network and to measure the passage time of a tracer through an open channel. All other measurements were performed using $\delta t = 0.005$. Reflective boundary conditions are used for chains in all directions (X, Y, Z), and for the c.m. of the tracer in X, Y directions.

We thank M. Elbaum for helpful conversations. Y.R. thanks A. Meller for hospitality during his stay at the Rowland Institute where part of this work was done.

This work was supported by a grant from the Israel Science Foundation. T.K. acknowledges financial support from the Coleman-Soref foundation.

REFERENCES

Allen, M. P., and D. J. Tildesley. 1987. Computer Simulation of Liquids. Clarendon Press, Oxford, UK.

Allen, N. P. C., L. Huang, A. Burlingame, and M. Rexach. 2001. Proteonomic analysis of nucleoporin interacting proteins. *J. Biol. Chem.* 276:29268–29274.

Ben-Efraim, I., and L. Gerace. 2001. Gradient of increasing affinity of importin β for nucleoporins along the pathway of nuclear import. *J. Cell Biol.* 152:411–417.

Bickel, T., and R. Bruinsma. 2002. The nuclear pore complex mystery and anomalous diffusion in reversible gels. *Biophys. J.* 83:3079–3087.

Chook, Y. M., and G. Blobel. 2001. Karyopherins and nuclear transport. *Curr. Opin. Struct. Biol.* 11:703–715.

de Gennes, P.-G. 1979. Scaling Concepts in Polymer Physics. Cornell University Press, Ithaca, NY.

Denning, P. D., S. S. Patel, V. Uversky, A. L. Fink, and M. Rexach. 2003. Disorder in the nuclear pore complex: the FG repeat regions of nucleoporins are natively unfolded. *Proc. Natl. Acad. Sci. USA.* 100:2450–2455.

Englmeier, L., J.-C. Olivo, and I. W. Mattaj. 1999. Receptor-mediated substrate translocation through the nuclear pore complex without nucleotide triposhate hydrolysis. *Curr. Biol.* 9:30–41.

Gilchrist, D., B. Mykytka, and M. Rexach. 2002. Accelerating the rate of disassembly of karyopherin-cargo complexes. *J. Biol. Chem.* 277:18161–18172.

Grest, G. S., and K. Kremer. 1986. Molecular dynamics simulation for polymers in the presence of a heat bath. *Phys. Rev. A.* 33:3628–3631.

Keminer, O., and R. Peters. 1999. Permeability of single nuclear pores. *Biophys. J.* 77:217–228.

Kremer, K., and G. S. Grest. 1990. Dynamics of entangled linear polymer melts: a molecular dynamics simulation. *J. Chem. Phys.* 92:5057–5086.

Lyman, S. K., T. Guan, J. Bednenko, H. Wordrich, and L. Gerace. 2002. Influence of cargo size on Ran and energy requirements for nuclear protein import. *J. Cell Biol.* 159:55–67.

Macara, I. G. 2001. Transport into and out of the nucleus. *Microbiol. Mol. Biol. Rev.* 65:570–594.

Nachury, M. V., and K. Weis. 1999. The direction of transport through the nuclear pore can be inverted. *Proc. Natl. Acad. Sci. USA.* 96:9622–9627.

Nevo, R., C. Stroh, F. Keinberger, D. Kaftan, V. Brumfeld, M. Elbaum, Z. Reich, and P. Hinterdorfer. 2003. A molecular switch between alternative conformational states in the complex of Ran and importin β1. *Nat. Struct. Biol.* 10:553–557.

Peters, R., E. Coutavas, and J. P. Siebrasse. 2003. Nuclear transport kinetics in microarrays of nuclear envelope patches. *J. Struct. Biol.* 140:268–278.

Rexach, M., and G. Blobel. 1995. Protein import into nuclei: association and dissociation reaction involving transport substrate, transport factors, and nucleoporins. *Cell.* 83:683–692.

Ribbeck, K., and D. Görlich. 2001. Kinetic analysis of translocation through nuclear pore complexes. *EMBO J.* 20:1320–1330.

Ribbeck, K., and D. Görlich. 2002. The permeability barrier of nuclear pore complexes appears to operate through hydrophobic exclusion. *EMBO J.* 21:2664–2671.

Rout, M. P., J. D. Aitchison, A. Suorato, K. Hjertaas, Y. Zhao, and B. Chait. 2000. The yeast nuclear pore complex: composition, architecture and transport mechanism. *J. Cell Biol.* 148:635–651.

Rout, M. P., and J. D. Aitchison. 2001. The nuclear pore complex as a transport machine. *J. Biol. Chem.* 276:16593–16596.

Salman, H., D. Zbaida, Y. Rabin, D. Chatenay, and M. Elbaum. 2002. Kinetics and mechanism of DNA uptake into the cell nucleus. *Proc. Natl. Acad. Sci. USA.* 98:7247–7252.

Schwoebel, E. D., B. Talcott, I. Cushman, and M. S. Moore. 1998. Ran-dependent signal-mediated nuclear import does not require GTP hydrolysis by Ran. *J. Biol. Chem.* 273:35170–35175.

Siebrasse, J. P., and R. Peters. 2002. Rapid translocation of NTF2 through the nuclear pore of isolated nuclei and nuclear envelopes. *EMBO Rep.* 3:887–892.

Stryer, L. (1995). Biochemistry. Freeman, New York, NY.

Suntharalingam, M., and S. R. Wente. 2003. Peering through the pore: nuclear pore complex structure, assembly and function. *Dev. Cell.* 4:776–789.

Vasu, S. K., and D. J. Forbes. 2001. Nuclear pores and nuclear assembly. *Curr. Opin. Cell Biol.* 13:363–375.